COMPARISON OF AAS, ICP-AES, PSA, AND XRF IN DETERMINING LEAD AND CADMIUM IN SOIL

by

Steven M. Pyle and John M. Nocerino
United States Environmental Protection Agency
Quality Assurance and Methods Development Division
944 E.Harmon Avenue
Las Vegas, NV 89119

Stanley N. Deming,John A. Palasota and Josephine M. Palasota
Department of Chemistry
University of Houston
4800 Calhoun Road
Houston,TX 77204-5641

Eric L. Miller,Daniel C. Hillman,
Conrad A. Kuharic, William H. Cole and Patricia M. Fitzpatrick
Lockheed Environmental Systems and Technologies Co.
980 Kelly Johnson Drive
Las Vegas, NV 89119

Michael A. Watson
Ecology and Environment, Inc.
1999 Bryan, Suite 2000
Dallas,TX 75201

Ky D. Nichols
United States Environmental Protection Agency
Region 6
1445 Ross Avenue, Suite 1200
Dallas, TX 75202-2733

ABSTRACT

Samples from a hazardous-waste site contaminated with lead and cadmium were analyzed by four independent laboratories, each using a different technique: atomic absorption spectroscopy (AAS), X-ray fluorescence (XRF) spectroscopy, inductively coupled plasma-atomic emission spectroscopy (ICP-AES) , and potentiometric stripping analysis (PSA) .

The four data sets were analyzed to: 11) establish the magnitudes of uncertainly in the measurements, (2) evaluate the comparability of the four instrumental methods, and (3) determine if any significant correlations exist between individual sets of data.

In general, the four techniques gave comparable results for the analysis of lead and cadmium, with the best agreement between PSA and AAS. Concentrations determined by PSA were higher than those measured by ICP-AES, AAS, and XRF, while concentrations determined by XRF were lower than, or equal to, recoveries determined by ICP-AES and AAS. Principal component analysis determined that the two major principal components in the sample space of the data set were analyte concentration and sample preparation.

The ICP-AES data were used to look for correlations among other elements in the samples. It was shown that concentrations of four of the elements (aluminum, zinc, iron, and calcium) were significantly higher than 19 other elements determined by ICP-AES. Principal component analysis on those 19 elements showed a first-component variation attributable to an analyte concentration effect and a second component variation attributable to an analyst-day effect.

The relative strengths and weaknesses of the four instrumental analysis methods, in relation to characterizing this particular hazardous-waste site, are discussed.

INTRODUCTION

The U. S. Environmental Protection Agency (U.S. EPA), Office of Research and Development (ORD), is continually investigating new technologies to improve existing methodology for the chemical characterization of hazardous waste sites. Many aspects of a new technology must be considered to determine its potential role for chemically characterizing a particular site or quantifying remediation effectiveness [l-3]. These considerations may include:

- Sensitivity,
- cost,
- simplicity/reliability,
- dynamic range of concentration,
- speed,
- accuracy,
- precision,
- utility,
- waste generation,
- field portability,
- ruggedness, and
- compatibility with existing EPA methods.

The final decision as to which technology or combination of technologies to use for site characterization must be based on a scientific comparison and careful analysis of each of those considerations.

Atomic absorption spectroscopy (AAS) and inductively coupled plasma-atomic emission spectroscopy (ICP-AES) [4] have been the EPA method of choice for the elemental analysis of soil extracts and aqueous samples because of their utility, sensitivity, and reliability. These methods can rapidly determine metals in trace amounts (after digestion) in many types of matrices. These methods are well-characterized and widely used, often for establishing analytical reference values for site samples.

In the course of initiating a hazardous site remediation two technologies, potentiometric stripping analysis (PSA) and X-ray fluorescence (XRF) spectroscopy, were evaluated for site characterization as alternatives or as additional methods to AAS and ICP-AES. The major site characterization objective was to determine the presence of lead and cadmium in soil samples.

XRF spectroscopy [4] is an established method that is just gaining popularity as a field-portable technique for environmental screening because it can provide rapid, multi-element measurements with minimal sample preparation. It is based on measuring the X-rays emitted from the elements in a sample upon irradiation with higher-energy X-rays (either from an X-ray tube or radioactive source). The energy levels of the emitted X-rays are characteristic of: the elements in the sample. The X-rays result from the interaction of the source X-rays with the inner-shell electrons of the elements in the sample, such that inner-shell electrons are ejected causing the higher-energy outer-shell electrons give up potential energy by filling the resulting holes and releasing energy in the form of X-rays.

PSA [5] is an electrochemical method that can identify and quantify metal ions in aqueous solutions. A thin mercury film, is plated onto a glassy carbon electrode by applying a reducing potential to the electrode while it is immersed in an aqueous mercury(II) chloride solution. The electrode is then placed into the solution to be analyzed and a fixed reducing potential is applied to reduce metal ions to the metallic form that will amalgamate into the mercury film. Reversing the potential will oxidize (strip) the metals back into solution as metal ions. At a fixed current, the resulting oxidation potential of the constant current working electrode is characteristic of the metal currently being stripped back into solution and the time the potential remains at any oxidation potential is proportional to the metal ion concentration.

In the course of site evaluation and remediation, 50 samples from a hazardous waste site contaminated with lead and cadmium were analyzed using an on-site AAS instrument and a Contract Laboratory Program (CLP) laboratory ICP-AES instrument. The results from these two instruments were compared with those resulting from the analysis of the same 50 samples using the two newer technologies, XRF and PSA. The objectives of this study were to examine the results from each instrument to: (1) establish the magnitudes of uncertainty in the measurements, (2! evaluate the comparability of the four instrumental methods, and (3) determine if any significant correlations exist between individual sets of data. These data are presented in Table I.

Collaboration for this study was begun after it became known that the four sets of data had already been collected. For this reason, a planned experimental design was not possible. Consequently, the four independent laboratories used four separate approaches to quality assurance, quality control, and calibration. This presented a challenge to the data analysis and limited the potential information that could be obtained from the 400 data points (50 samples x 4 techniques x 2 analytes) collected from this Superfund site. Nevertheless, the data

collected during the remediation project represented a real-world
situation and a unique opportunity for a comparison of the four
techniques.

Figure 1 shows the sample treatment scheme for the 50 soil samples. The samples were collected at an industrial hazardous waste site and split into duplicate portions. The first portion was divided into two sub-portions. One sub-portion was digested for on-site AAS analysis, and the other was sent to the XRF laboratory where it was dried, sieved, and homogenized prior to XRF analysis. The second portion was sent to the ICP-AES laboratory for digestion and subsequent analysis. The remaining AAS laboratory digestate was sent to the PSA laboratory for analysis.

XRF. X-ray fluorescence analysis was performed on an X-MET 880 XRF instrument (Metorex, Bend, OR). Subsamples of the 50 soil samples were dried, sieved, homogenized, and further subsampled into SPEX X-ray cells. Calibration curves were made from the confirmatory CLP AAS data using the americium 241 (^{241}Am) source for the determination of cadmium and the curium 244 (^{244}Cm) source for the determination of lead. Ten samples over the analytical range were selected from the 50 original samples and used to construct this calibration curve. The 50 samples were re-measured against this calibration curve as unknowns.

Digestion. The 50 soil samples were digested using EPA Method 3050 [6] for subsequent analysis by AAS, ICP-AES, and PSA. A l-to-2-g portion of soil was weighed into a beaker followed by addition of 10.0 mL of 1:l $HNO_3:H_2O$. This solution was heated to 95 ^{0}C for 5 min, followed by sequential addition of 5.0 mL of concentrated HNO_3, 1.0 mL of 30% H_2O_2, and 5.0 mL of concentrated Hcl. The resulting solution was filtered and diluted with deionized water to a final volume of 100.0 mL.

AAS. Atomic absorption spectroscopy was performed on a Buck Scientific, Model 200A Single-Beam AA Spectrophotometer using EPA Method 7130 [6] (for cadmium) and EPA Method 7420 [6] (for lead). The manufacturer lists the detection limit for lead at 0.05 µg/mL, with a working range of 2.5 to 20 µg/mL at 217 nm, and the detection limit for cadmium at 0.002 ug/mL, with a working range of 0.2 to 1.8 µg/mL at 228.8 nm.

ICP-AES. Inductively coupled plasma-atomic emission spectroscopy was performed on a Thermo Jarrell Ash, Model Enviro 36, ICP-AES using EPA Method 6010 [61. The samples were analyzed over a two-day period with blanks, initial and continuing calibration verification standards, and ICP interference check samples run tar each batch of ten environmental samples that were analyzed.

PSA. Potentiometric stripping analysis was performed on a Radiometer TraceLab system (Radiometer, Westlake, OH), comprising a PSU20 potentiometric stripping unit, a SAM20 sample station, and three electrodes [7] The PSU20 includes a potentiostat, current generator, and signal processor. The SAM20 is a manually-operated electrode holder and sample stand. The electrodes include a P136 platinum counter electrode, a K436 saturated-calomel reference electrode (SCE), and an F3600 glassy-carbon working electrode (GCE). The system is controlled by a personal computer, using Radiometer programming software. The electrode-plating solution contained 38 mg/L of mercury in 0.062 M HCl.

The CCE was cleaned by wiping with a paper towel, brightened with polishing powder, and then rinsed with water. The electrodes were immersed in the plating solution and the plating program was initiated. After the program was completed, the electrodes were removed from the plating solution and rinsed with water. When not in use, the electrodes were stored in water.

Dissolved lead and cadmium in the 50 sample solutions were quantified by the method of standard additions using 2 additions. The electrodes were rinsed with water and then immersed in a polypropylene beaker containing about 30 mL of the sample to be analyzed. The quantitation program was initiated. After the first analysis was completed, the sample in the beaker was spiked with standard lead and cadmium solutions, and the spiked sample was analyzed. The spiking and analysis procedures were performed two times. After the analyses were complete, the electrodes were removed from the solution and rinsed with water.

RESULTS AND DISCUSSION

Correlation Diagrams

Figures 2 and 3 show multiple two-factor correlation plots (bivariate scatter diagrams) between each instrumental method for lead and cadmium concentrations, respectively. In each plot, the solid lines are the coordinate axes. If the lead (Fig. 2) and cadmium (Fig. 3) concentrations by the methods along the x- and y-axes were perfectly correlated, all of the data points would lie along the dashed line going from the lower left to the upper right.

The first row in each figure shows plots of the ICP-AES versus the AAS, PSA, and XRF results. The second row shows plots of the AAS versus the PSA and XRF results. The third row shows a plot of the PSA versus the XRF results.

There seem to be two populations of lead data in the ICP-AES comparisons (the first row of panels in Figure 2). In the first, population (nearly parallel to the y-axis), the lead recoveries using the ICP-AES method are greater than those obtained by any of the other analyses; in the second population (closer to the dashed line), the lead recoveries using the ICP-AES method are lower than those of the other methods.

In general, the lead recoveries using the PSA method are higher than the lead recoveries using the ICP-AES, AAS, and XRF methods. The lead recoveries using the XRF method are lower than, or approximately equal to, the lead results using the ICP-AES and AAS methods.

In Figure 3, cadmium results using the ICP-AES, AAS, and PSA methods seem better correlated than the lead recoveries in Figure 2. In general, cadmium results using PSA are slightly higher than recoveries using ICP-AES or AAS.

Principal Component Analysis on Lead and Cadmium Recoveries

Since these were not experimentally-designed experiments, a multivariate exploratory data analysis technique, namely, *principal component analysis* (PCA), was used to statistically evaluate the results. PCA is exploratory in the sense that it helps to generate hypotheses from collected data. This is different from experimental design studies, which test hypotheses on data about to be collected. There are several reasons to consider PCA when exploring a data set:

- to gain a better understanding of the relationships among the variables,

- to reveal groups or clusters of observations,

- to reveal outlier values ("outliers"),

- to reduce the dimensionality of the data,

- to possibly identify a physical meaning from the principal components,

8

- to estimate the nonsystematic variance (from random error and irrelevant variables), and

- to achieve a better feel for the "structure" of the data set.

Variables that depend on "similar intrinsic properties" may be described by a principal property represented by a single "new" variable. If the data for a variable can be calculated from the data from any of the other variables, then there exists redundant information. There should be no (or little) loss of information by representing that portion of redundant data with this "new" variable (of course, this "new" variable was there all along.) If there are variables that are linearly correlated, and, therefore, not linearly independent, then the dimension-ality of the data set may be reduced by using a smaller number of linearly independent "new" variables. These new variables are the principal *components* (PCs), each of which is a linear combination of the original correlated variables. Principal component analysis qives valuable insight about this correlated structure of the data.

The PCs are found by rotating the original coordinate axes in variable space such that the first PC describes the vector through the maximum systematic variation in the data set. The second PC describes the second largest variation in the data set by d vector orthogonal to the first PC. For each PC, an eigenvalue is derived from the data set. This eigenvalue is proportional to the variance described by that PC. This process is continued until all (or most all) of the systematic variation in the data set has been described by the PCs.

Since the first PC is orthogonal to the second PC (they are uncorrelated), each PC should describe different underlying principal properties or components. Thus, observations with similar principal properties should group (cluster) together in the PC space. An observation that does not distinctly exhibit any of the principal properties may be considered an outlier. The location of a data point of an object for a particular PC in this transformed component space is given by the data point's score. Score plots of one PC versus another PC can quickly reveal clusters of objects or outliers.

The loading of a variable on a PC is a result of the rotation of the original data into the principal component space. These loadings have the elements of the cosines between each variable vector and principal component eigenvector. Thus, the more that a variable contributes to a principal component, the larger (approaching unity) its loading will be. The sign of the

loading indicates if the variable-component angle is obtuse (negative value) or acute (positive value). Inspecting the loading values is a rapid means of distinguishing between the relative contributions of important variables.

Principal component analysis [8,91, using the singular value decomposition method [l0], was applied to the combined data. The PC of analytical methods in sample space accounts for the majority of the variation in the lead and cadmium data (see Table II and III, respectively). This can be attributed to a concentration effect. Note that all of the loading values for the first principal component in Tables IV and V are about the same magnitude, indicating that each variable (the four different analytical methods) contributes about equally to the first PC.

Figures 4 and 5 show the PCA score plots for the lead and cadmium data, respectively. Each filled symbol represents an off-site analysis, and each open symbol represents an on-site analysis. For the lead data (Figure 4), all four methods agree fairly well as indicated by the single, moderately tight, clustering of the symbols; however, the first principal component. (PCl) for the PSA off-site analyses has a greater scalar magnitude than the other three methods. This suggests that the ?SA method shows a greater recovery for lead than the other three methods [10].

For the cadmium data (Figure 5), the ICP-AES, AAS, and PSA methods agree fairly well. The first principal component (PCl) for the XRF on-site method, however, has a slightly greater magnitude than the other three. This greater magnitude ("concentration effect") suggests that the XRF method shows a greater recovery for cadmium than the other three methods [10].

The second principal component (PC2) for the XRF on-site method for cadmium also has a greater magnitude than the other three. Because PC1 accounts for over 90 percent of the systematic variation (Table III), the outlying score in PC2 implies that XRF has a different random (experimental) error component for the determination of cadmium than do the other methods.

Relationships within the ICP-AES Data

Principal component analysis can be used to discern differences in results based on an analyst-day bias. A review of the ICP-AES data revealed that two different researchers analyzed the samples, each on a different day (the change in analyst and change in day are, for the most part, confounded).

Figure 6 shows the PCA results of samples in technique space for all of the 23 elements analyzed by ICP-AES. Each filled circle corresponds to samples analyzed on one day by analyst "A" (day 1 with the exception of one sample on day 2), and each open circle corresponds to samples analyzed by analyst "B" (day 2). The separation of the filled and open circles in Figure 6 indicates that the results are analyst-day dependent.

Figure 7 shows the relationships among the results for each element. The results of four (aluminum, calcium, iron, and zinc) of the 23 elements appear to be different from the remaining 19. Thus, it appears that the soil samples are different In aluminum, calcium, iron, and zinc content compared with the other elements detected. Since these cations are naturally abundant, they would also be expected to be among the most abundant elements in blank (nearby, uncontaminated) soils if analyzed by these methods.

Because of the extremely high levels at which they are present, it is probable that aluminum, calcium, iron, and zinc had a strong influence on the PCA results and masked the effects of other elements. The data associated with those four elements were removed and PCA was performed on the remaining subset of data. In Figure 8, results from analyst "B" (day 2) appear to be more spread out in the second principal component direction than results from analyst "A." Again, it appears that the results are analyst-day dependent. That is, variation in the first PC may be due to a concentration effect and the second PC most likely contains an analyst-day effect.

Outlier Detection

Determining outliers is also an important exploratory statistical technique used to analyze and gain information from a data set (Barnett and Lewis). Multivariate outliers were searched for in the lead methods data using the Mardia's kurtosis algorithm [11] at the alpha 0.05 level. Twenty of the 50 observations (samples) were found to be discordant (outliers), as displayed in Table VI. The variables (methods) responsible for causing those discordancies, generated by the causal variable algorithm [11], are given in Table VII. The expected values for those observations are also given in Table VII. Most of the discordancies are magnitude outliers, due to those samples that contained more lead. However, several large trend-outliers were found more frequently due to the ICP-AES method. A notable ICP-AES outlier is from sample E4B. This may have been a dilution error since 1252 ppm Pb was observed, which is roughly a factor of ten higher than expected (115 ppm). These outliers reflect the two different populations for the ICP-AES lead data in Figure 2. Causes for these outliers should be explored in future

<u>experiments.</u>

Sample versus Lead and Cadmium Results

Although there are uncertainties associated with the analyses of the 50 samples by the four techniques, all four techniques gave adequate analytical results. This point is illustrated by plots of the lead analysis versus sample for the four techniques (Fig. 9) and the cadmium analysis versus sample for the four techniques (Fig. 10). With the exception of the trend outliers, especially for the ICP-AES lead data, it can be seen that the techniques generally agree.

The combined cadmium results are not as precise as the lead results; nonetheless, the cadmium recoveries for the techniques, except for possibly the XRF results, are in fair agreement. Also, the XRF cadmium results show a positive bias compared with the other techniques.

It should be noted that there is less variation between the .&AS results and the PSA for both the lead and cadmium results because they were performed on the same sample digestates.

DISCUSSION AND CONCLUSIONS

While each of the four instrumental techniques could be used to adequately characterize the site, the final choice of which technique, or techniques, to use must be based on the relative importance of factors, such as cost, sensitivity, speed, precision, and utility of the technique.

For example, while the XRF method had larger residuals about the average of all of the compared methods, XRF would be considerably faster and less expensive since it does not require extensive sample pre-treatment and is field portable. XRF would, therefore, be particularly valuable as a screening tool for the determination of "hot spots" at a field site.

The PSA method should be considered as a viable alternative because it is also field portable like the XRF method (although PSA would require an on-site digestion), yet has a sensitivity and residuals similar to the ICP-AES and AAS methods.

The ICP-AES and AAS methods show smaller residuals for lower levels of contamination.

The analysis of soil samples by the AAS, ICP-AES, PSA, and XRF methods offered a unique opportunity to contrast and compare the techniques. Usually, the evaluation of a method or technique is accomplished using spiked samples or standards in relatively pure solutions under highly-controlled conditions. Such conditions demonstrate the potential of the method or technique

13

only in a best-case scenario. In the case of real-world environmental samples, however, all variables are not under the control of the analyst [ll]. For example, there may be little knowledge of potential interferences or concentration levels. The environmental samples analyzed and reported here give a more realistic indication of the relative utility of each of the four techniques.

ACKNOWLEDGMENT

REFERENCES

1. A. L. Wilson, "The Performance-Characteristics of Analytical Methods-I," *Talanta*, **17**, 21-29 (1970).

2. A. L. Wilson, "The Performance-Characteristics of Analytical Methods-II," *Talanta*, **17**, 31-44 (1970).

3. A. L. Wilson, "The Performance-Characteristics of Analytical Methods-III," *Talanta*, **20**, 725-732 (1973).

4. D. A. Skoog, *Principles of Instrumental Analysis*, 3rd ed. (New York: Saunders, 1985).

5. A. J. Bard and L. R. Faulkner, *Electrochemical Methods: Fundamentals and Applications* (New York: Wiley, 1980).

6. U.S. EPA Methods 3050, 7130, 7420, *Test Methods for Evaluating Solid Waste: Laboratory Manual-Physical/Chemical Methods. SW-846*, 3rd ed. (Washington, DC: U.S. EPA, November 1986).

7. E. L. Miller, "Quantifying Lead and Cadmium in Aqueous Solutions by Potentiometric Stripping Analysis," *U.S. Environmental Protection Agency*, **EPA/600/X-91/114**, August 1991.

8. J. E. Jackson, *A User's Guide to Principal Components* (New York: Wiley, 1991).

9. S. J. Gould, *The Mismeasure of Man* (New York: Norton, 1981).

10. R. Carlson, *Design and Optimization in Organic Synthesis* (Amsterdam: Elsevier, 1992), pp. 426-427.

11. M. A. Stapanian, F. C. Garner, K. E. Fitzgerald, G. T. Flatman, and J. M. Nocerino, "Finding Suspected Causes of Measurement Error in Multivariate Environmental Data," *J. Chemometrics*, **7**, 165-176 (1993).

Table I. Lead and cadmium concentrations in the 50 soil samples as determined by the four methods of ICP-AES, AAS, PSA, and XRF.

sample	LEAD (mg/kg)				CADMIUM (mg/kg)			
ID	ICP-AES	AAS	PSA	XRF	ICP-AES	AAS	PSA	XRF
A1	57.13	46.51	50.35	46	0.83	10.35	21.51	15
A2	76.13	76.02	105.28	26	0.85	6.88	6.38	57
A3	51.55	34.02	202.99	20	0.79	8.05	10.09	3
A4	61.77	69.67	77.34	133	1.36	8.71	8.24	43
A5	27.33	33.85	33.17	10	0.78	3.84	3.38	34
A6	38.86	45.67	52.98	34	17.41	5.82	9.48	41
B1	32.96	45.28	43.02	17	0.77	6.79	4.98	24
B2	1398.58	1757.57	2671.02	1092	4.58	25.44	31.80	44
B3	52.42	70.48	76.70	5	16.31	8.22	5.87	22
B4	10.36	112.36	122.02	11	0.84	11.83	10.96	15
B5	42.03	70.09	85.75	16	14.02	5.48	7.94	36
B6	70.22	54.84	31.81	84	42.1	3.29	2.98	13
C1	243.83	303.81	307.47	186	28.75	33.42	38.65	10
C11	254.57	101.64	99.38	0	13.64	9.82	20.55	16
C2	735.89	978.09	1254.18	720	85.52	97.52	117.94	135
C31	1274.97	1496.37	1635.39	1504	103.54	122.38	152.85	57
C32	752.63	993.39	1107.30	909	31.68	49.22	68.54	26
C33	204.84	197.1	281.74	136	36.7	22.03	19.48	21
C4	111.32	149.67	88.42	55	19.68	13.13	10.48	55
C41	66.08	10.74	109.54	170	19.22	23.41	44.25	47
C5	38.32	57.92	47.73	34	0.78	6.02	4.87	39
C6	33.23	45.04	37.72	0	0.77	5.52	4.28	47
D1	64.23	61.29	97.21	45	0.83	6.13	11.16	41
D2	62.95	44.37	83.42	2	0.79	7.43	9.98	21
D3	300.95	448.88	390.86	303	37.01	20.91	22.12	33
D4	1869	2335.02	2845.15	2253	190	223.3	212.04	220

16

D41	125.39	155.43	216.50	145	38.57	16.99	16.76	57
D4A	85.86	36.83	92.07	60	17.12	14.45	16.48	11
D4B	59.01	71.41	83.86	20	19.61	14.79	16.73	31
D5	48.94	48.85	65.17	2	23.93	4.98	2.34	1
D61	31.44	11.91	54.07	0	14	5.36	5.95	53
D62	281.73	34.07	48.94	0	12.06	5.45	5.00	42
E1	47.19	57.7	66.82	9	0.83	4.62	4.15	30
E2	33.64	20.99	82.92	0	0.73	3.57	1.59	43
E3	85.3	96.15	113.57	18	26.38	13.3	12.83	42
E4A	82.29	96.39	83.53	91	18.18	10.28	12.32	47
E4B	1252.12	112.99	135.58	83	20.43	7.91	13.22	41
E5	68.41	62.45	69.42	27	26.02	5.41	5.83	18
E6	493.15	81.51	71.96	9	19.26	5.82	7.45	33
F1	343.29	451.09	549.00	170	5.76	15.95	24.20	49
F2	75.84	62.97	57.82	6	12.58	2.81	1.95	34
F3A	4.81	32.69	44.46	18	1.85	3.92	3.60	67
F3B	50.92	31.73	43.05	9	18.37	6.35	5.08	34
F4	4.76	21.7	24.30	0	37.36	3.69	1.19	29
F5	30.26	31.99	31.88	2	13.57	3.41	2.77	37
F6	43.49	23.92	32.89	14	13.25	3.59	24.16	27
X1	8.4	29.22	18.13	46	6.1	2.48	3.51	38
X2	4.03	13.87	69.08	18	5.02	2.64	2.36	42
Z1	363.45	32.72	31.20	22	0.75	3.05	1.96	58
Z2	299.54	35.45	146.51	28	17.08	4.96	42.89	26

Table II. Lead recovery (ppm) data principal component analysis.

	Square Root	Eigenvalue	Cumulative Eigenvalue	Percent
PC 1	7.3324×10^3	5.3764×10^7	5.3764×10^7	95.9522
PC 2	1.2482×10^3	1.5580×10^6	5.5322×10^7	2.7805
PC 3	8.0652×10^2	6.5047×10^5	5.5973×10^7	1.1609
PC 4	2.4414×10^2	5.9603×10^4	5.6032×10^7	0.1064

Table III. Cadmium recovery (ppm) data principal component analysis.

	Square Root	Eigenvalue	Cumulative Eigenvalue	Percent
PC 1	6.2257×10^2	3.8759×10^5	3.8759×10^5	90.0324
PC 2	1.8669×10^2	3.4853×10^4	4.2244×10^5	8.0960
PC 3	7.9940×10^1	6.3904×10^3	4.2884×10^5	1.4844
PC 4	4.0827×10^1	1.6668×10^3	4.3050×10^5	0.3872

3

Table IV. The loadings matrix for the lead recovery (ppm) data.

	ICP-AES	AAS	PSA	XRF
PC 1	-0.42047	-0.49790	-0.62891	-0.42400
PC 2	0.90695	-0.20761	-0.30694	-0.20032
PC 3	0.00663	-0.05752	0.58601	-0.80824
PC 4	0.02461	-0.84005	0.40848	0.35616

Table V. The loadings matrix for the cadmium recovery (ppm) data.

	ICP AES	AAS	PSA	XRF
PC 1	-0.41390	-0.44346	-0.48282	-0.63160
PC 2	0.27652	0.39080	0.41564	-0.77334
PC 3	-0.83821	0.13662	0.52542	0.05172
PC 4	0.22277	-0.79495	0.56397	-0.01895

Table VI. For the lead samples, 20 of the 50 observations were
found to be discordant using the Mardia's kurtosis
algorithm [11] (alpha = 0.05).

Observation No.		Kurtosis	P-Value
B2	96.78		< 0.005
E4B	79.16		< 0.005
D31	64.91		< 0.005
C31	67.20		< 0.005
C32	65.42		< 0.005
C2	67.56		< 0.005
F1	59.18		< 0.005
D3	57.01		< 0.005
C1	53.46		< 0.005
C41	51.48		< 0.005
E6	48.92		< 0.005
Z1	48.98		< 0.005
A3	50.56		< 0.005
Z2	49.89		< 0.005
D62	52.15		< 0.005
C11	54.12		< 0.005
B4	47.47		< 0.005
C33	43.34		< 0.005
D41	43.55		< 0.005
A4	38.51		< 0.0112

0 of the 50 observations are missing
20 of the 50 observations are discordant

After removing the 20 discordant observation(s),
the test statistic is 36.16 with a P-Value of 0.07

Table VII. The variables (i.e., methods) responsible for causing discordancies in the lead data and the expected values for those observations.

Obs. No.	Test	PValue	Variable	Observed	Expected	Low Lim	Up Lim
A3	25.36	0.07	PSA	202.99	61.242	13.974	108.504
A4	25.35	0.07	ICP AES	61.77	91.929	43.735	140.124
	25.19	0.08	AAS	69.67	74.115	16.217	132.014
	24.76	0.11	XRF(Qm)	133.0	26.062	-25.323	77.448
B2			None				
B4	25.44	0.06	ICP AES	10.36	99.281	56.268	142.293
	24.87	0.1	AAS	112.06	30.704	-25.814	87.223
C1			None				
C11	25.53	0.06	ICP-AES	254.57	78.381	41.237	115.524
C2			None				
C31			None				
C32			None				
C33			None				
C41	24.4	0.14	XRF(Qm)	170.0	11.483	47.47	73.436
D1			None				
D31			None				
D41			None				
D62	24.15	0.16	ICP AES	281.73	32.198	-3.147	57.542
E4B	23.82	0.2	ICP-AES	1252.12	115.358	73.488	157.229
E6	25.06	0.09	ICP-AES	493.15	64.926	28.714	101.138
F1			None				
G1	24.09	0.17	ICP-AES	363.45	26.002	-11.224	63.227

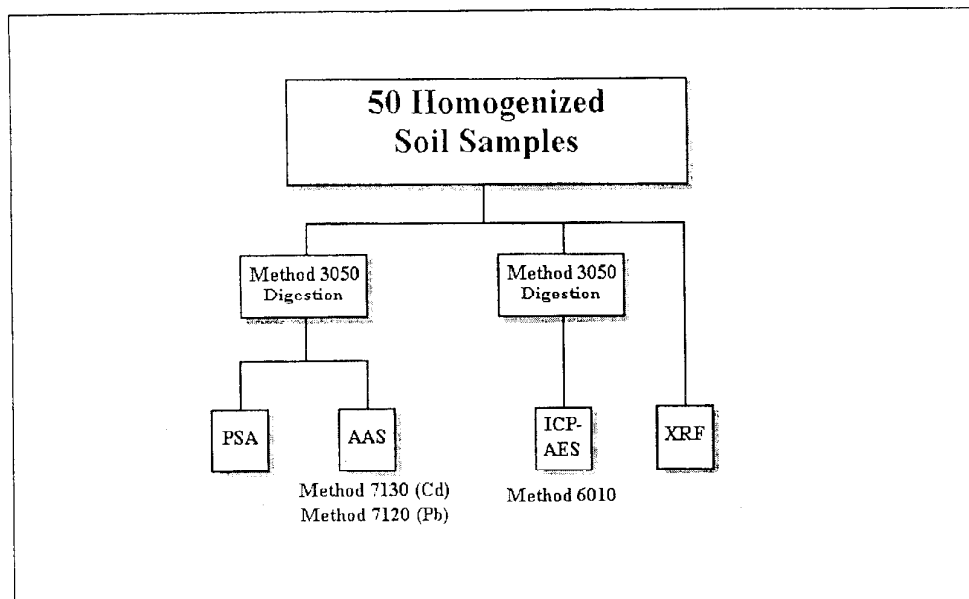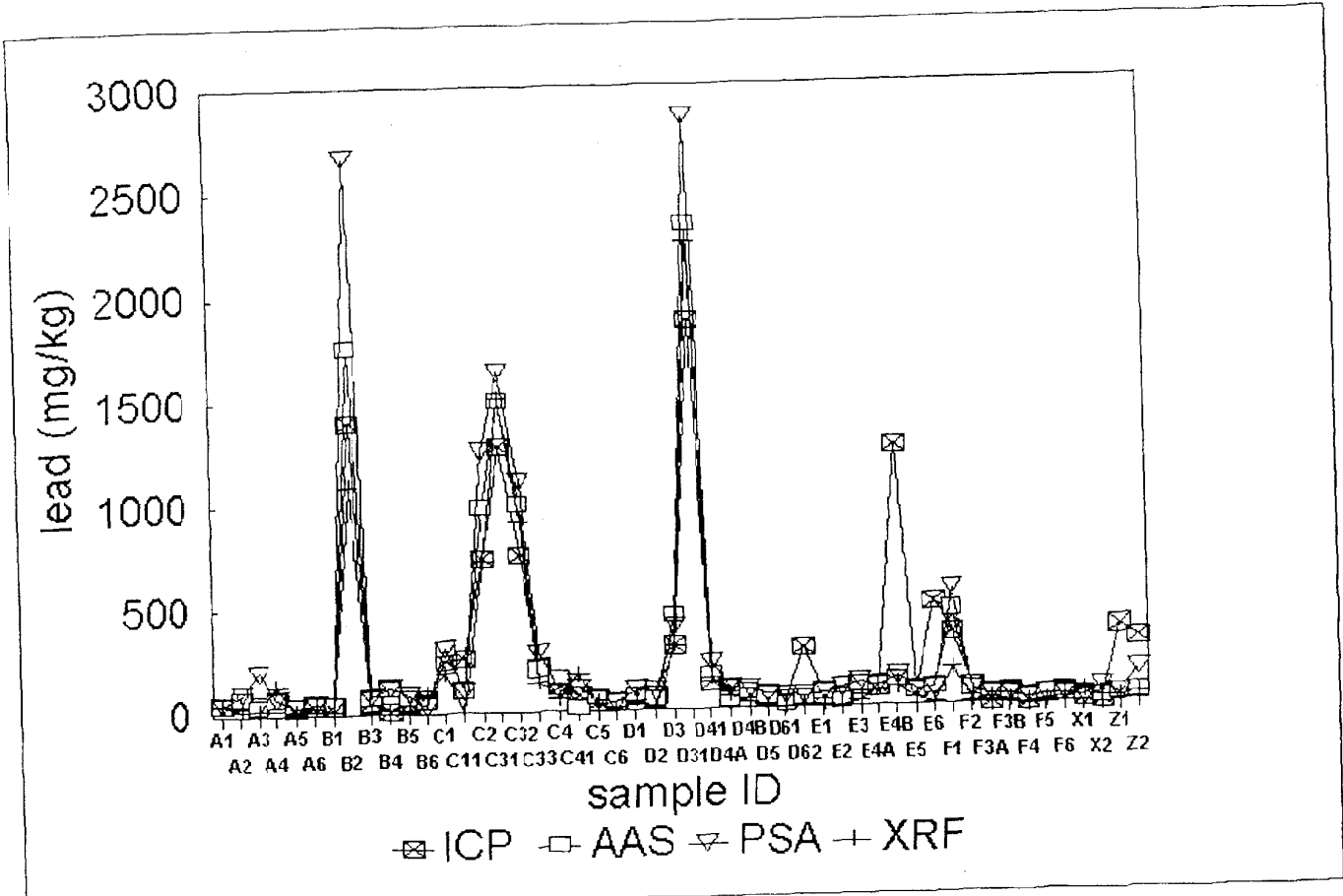22   None

LIST OF FIGURES

Figure 1. Sample treatment scheme

Figure 9.

THIS PAGE WAS LEFT BLANK

Figure 10.